Saccadic Suppression Enhances Saliency of Prey-Like Stimuli in the Optic Tectum

Giulia Soto[1], Carina Thomas[1], Tim C. Hladnik[1,2], Florian A. Dehmelt[1], Ziad M. Hafed[1,3], Aristides B. Arrenberg[1,*]

[1]Werner Reichardt Centre for Integrative Neuroscience, University of Tübingen, Tübingen, Germany

[2]Graduate Training Centre of Neuroscience, University of Tübingen, Tübingen, Germany

[3]Hertie Institute for Clinical Brain Research, University of Tübingen, Tübingen, Germany

*e-mail: aristides.arrenberg@uni-tuebingen.de

Abstract (200 words)

Saccadic suppression, a reduction in visual sensitivity around the time of a rapid eye movement, is a robust perceptual phenomenon, extensively studied in primate psychophysics. However, the mechanisms and purpose of saccadic suppression are still debated in the field. Here, we demonstrate saccadic suppression in zebrafish, and trace its origins not only in retinal circuits, but also in downstream visual and motor-related neurons of the optic tectum. Using electrophysiology, we first established that retinal ganglion cells jumpstart saccadic suppression, in a spatial frequency dependent manner. Calcium imaging of the optic tectum, combined with 360° visual stimulation and behavioral tracking, revealed that motor signals enhance peri-saccadic suppression strength up to 0.5 s after the saccade. Notably, vision-mediated saccadic suppression lasts more than 3 s. Suppression strength depends on saccade size. Interestingly, we found much weaker saccadic suppression in the optic tectum for stimuli related to hunting behavior than for behaviorally less relevant global flashes, suggesting a selectivity of saccadic suppression aimed at increasing the salience of particular types of visual stimuli after saccades. These findings demonstrate that saccadic suppression in zebrafish integrates visual and motor signals to optimize sensory processing within neural constraints, providing insights into evolutionarily conserved visual strategies.

Introduction

Saccadic eye movements are an efficient way of rapidly sampling the visual environment, employed by many species across the animal kingdom. However, by moving the eyes at several hundred degrees per second from one direction of gaze to another, visual flow is greatly disrupted, a disruption that we are blissfully unaware of in our daily perception. From a perceptual standpoint, this can be explained through a phenomenon known as saccadic suppression. Saccadic suppression describes a brief peri-saccadic reduction in perceptual sensitivity and it has been investigated in primates for decades[1–5]. Physiological studies furthermore showed that individual neuronal responses in visual areas are concomitantly reduced peri-saccadically[5], and that responses to stimuli of lower spatial frequency are suppressed more strongly[3,6]. While the benefit of suppressing visual processing during saccades intuitively makes sense, its computation in the brain as well as the reasons underlying variable suppression strengths under different image conditions are still unclear.

Zebrafish (*Danio rerio*) offer the opportunity to investigate neural correlates of saccadic suppression across the visual system in a vertebrate "blueprint" brain without a visual cortex. Larval zebrafish start exhibiting spontaneous saccadic eye movement prior to 4 days post-fertilization (dpf); by 5 dpf, saccades are well coordinated and comparable to adults[7]. Moreover, brainstem control of saccadic eye movements is highly conserved across evolutionarily distant species like zebrafish and primates[8]. Finally, the optic tectum (OT) of zebrafish is homologous to the primate superior colliculus (SC), and both of them are highly sensitive to visual stimulation[9]. Thus, zebrafish are well suited to answer the long-standing debate in the field on the origins and purposes of saccadic suppression.

Considering the frequent occurrence of saccadic eye movements, it might be naïve to think that saccadic suppression simply serves the purpose of suppressing a visual disturbance. Suppression of visual information for fractions of a second with every executed saccade seems simply like too large of a loss

of sensory information, particularly in a system strapped for neural resources, such as the small larval zebrafish brain. A potential purpose of saccadic suppression could, instead, be as a precise tool for efficient task-specific encoding. The observation that visual stimulus properties affect suppression dynamics would be in line with this possibility. For example, saccades across low spatial frequency surroundings will lead to stronger and longer lasting suppression, compared to high spatial frequency surroundings[6,10–12]. Similar effects can be observed with luminance contrast dependency[6,13] and chromatic contrast[14]. Thus, saccadic suppression can be highly specific and depends on image content. As we show here, the stimulus-dependence of saccadic suppression could even be beneficial to optimize sensory encoding in behavioral contexts, such as prey capture, where saccadic eye movements play a vital role in the behavioral sequence[15].

The preponderance of evidence for visual dependencies of saccadic suppression both illuminates and complicates the search for the circuit origins of saccadic suppression. For example, is saccadic suppression purely visual? Masking, or the reduced visibility of one brief visual stimulus due to the presence of a second brief visual stimulus[16], plays a vital role in generating saccadic suppression. In the 1970's, there was already behavioral evidence that visual masking leads to the reduced perception of a "blur", a visual disturbance caused by the saccadic eye movements itself[17,18]. More recently Idrees and colleagues showed in isolated mammalian retinae, that visual masking leads to reduced responses to a probe flash in retinal ganglion cells, following a saccade-like texture displacement[6,19]. However, saccadic motor signals still likely play a role. For example, it is known from psychophysics studies that the peri-saccadic window of suppression was significantly shortened[6] when participants performed real saccades instead of watching a simulated corresponding visual stimulus (a texture displacement). Corollary discharge signals originating from motor commands can act as inhibitory signals for visual neurons during rapid eye movements[4,20]. Recent work by Ali and colleagues has shown that for locomotion, a

corollary discharge signal can in fact be found in the zebrafish OT, the sensory structure responsible for processing most visual inputs in the zebrafish brain[21]. In primates, behavioral and neuronal evidence suggest the presence of a saccade-related corollary discharge signal in parts of the visual system[22–25].

It is evident that both visual and motor-related signals shape saccadic suppression properties. However, how the two act together on the individual neuronal level to modulate visual responses is poorly understood. Here, we show in larval zebrafish how visual responses of tectal neurons are modulated by sensory and motor-related signals during peri-saccadic suppression, by imaging large populations of OT neurons through calcium imaging, while simultaneously using 360° whole-field visual stimulation and behavioral tracking in tethered animals. We find that both visual and motor related processes shape saccadic suppression differentially in the OT. The optic tectum receives purely visually suppressed signals from the retina and further modulates them. Motor-related signals in the OT enhance saccadic suppression. Furthermore, stimuli related to hunting behavior appear more salient, because they are less suppressed than behaviorally irrelevant global flashes, indicating optimized signal processing.

Results

Purely visual saccadic suppression exists in the zebrafish retina

To enable our investigation of peri-saccadic stimulus encoding, we first need to demonstrate that saccadic suppression does exist in zebrafish. We started with recording in the retina, because this is the location where saccadic suppression first occurs in the mammalian visual system[6]. Thus, we isolated adult zebrafish retinae and performed multi-electrode array (MEA) recordings of retinal ganglion cells (RGCs) during visual stimulation (Fig. 1a). In order to simulate the visual transient of a saccade, retinae

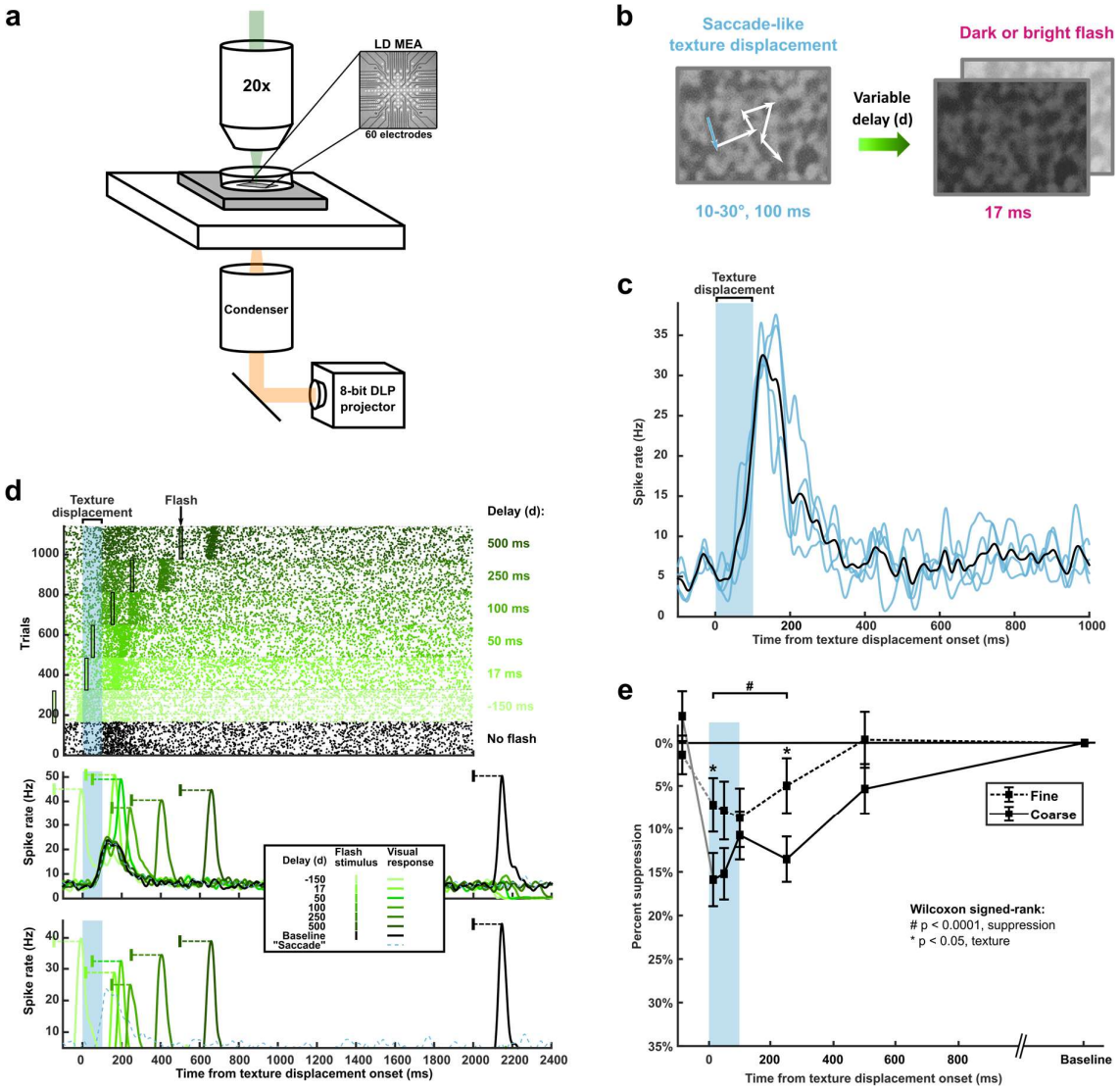

Fig. 1. Visual saccadic suppression in zebrafish retinae. a. RGC activity of adult zebrafish retinal explants was recorded on low-density multi-electrode array (LD MEA) with simultaneous visual stimulation with DLP projector from below. **b.** Textured stimulus was rapidly displaced in a saccade-like manner (blue arrow). After a variable delay period (d), a whole-field dark or bright flash was shown. **c.** Average spike rate (black line) to texture displacement of example RGC across multiple trials (blue lines). Blue bar indicates time span of texture displacement. **d.** Spike count for individual trials (upper panel) and average spike rate across trials (middle panel) for the same example RGC as in **c,** when texture displacement was paired with a whole-field flash after various delay periods. Isolated flash responses (lower panel) were acquired by subtracting "saccade" activity (blue dashed line) from flash activity (solid green lines). Green bars indicate time points of flash presentation; gray bar indicates time span of texture displacement. **e.** Percent suppression (mean ± SEM) of visual responses to whole-field flash around the time of a saccade-like texture displacement (gray bar) across all RGCs recorded. RGC activity was significantly suppressed during and up to 250 ms after texture displacement onset (# $p < 0.0001$, two-tailed Wilcoxon signed-rank test). Suppression was significantly stronger for coarse textures, than fine (solid vs. dashed line), where indicated by asterisk (* $p < 0.05$, two-tailed Wilcoxon signed-rank test, Bonferroni corrected for n = 18 conditions (6 delays vs. baseline for coarse texture, 6 delays vs. baseline for fine texture, 6 coarse vs. fine texture at each delay time)). *N = 87 RGCs from 10 animals.*

113 were shown a coarse or fine texture which was rapidly displaced in a saccade-like manner (Fig 1b, left).
114 Texture displacements generated a visual response in RGCs as can be seen in Fig. 1c. To test if saccade-
115 like texture displacements could suppress responses of a secondary visual stimulus, at various time
116 points in close temporal proximity to the texture displacement, a 17 ms long dark or bright whole-field
117 flash was shown (Fig. 1b, right, Fig. 1d). Flash responses, when shown in temporal isolation ("Baseline")
118 were robust and in most cases much larger than texture displacement responses. In order to isolate
119 flash-associated responses around the time of the texture displacement, texture displacement-associated
120 responses were subtracted from flash responses as shown in Fig. 1d (second and third panel). After
121 removal of this "saccade"-associated response it can be seen that flash responses are significantly
122 suppressed around the time of the texture displacement (Fig, 1d, third panel). When averaging all RGCs
123 recorded (n=87), it became apparent that suppression is strongest at 17 and 50 ms after texture
124 displacement onset and that responses return to baseline levels after ~300 ms (Fig. 1e). This is a similar
125 time course to that described in mouse and pig retinae[6]. Overall suppression strength is, however,
126 weaker in zebrafish, with a maximal suppression of 15.8 ± 3.0% (mean ± SEM), whereas mammalian
127 retinal saccadic suppression can be as strong as ~30% (see Ref. 19, Fig. 3). Furthermore, when
128 comparing the suppression induced by a coarse texture displacement versus a fine texture displacement,
129 coarse will generally lead to stronger and longer lasting suppression, than fine, reproducing spatial
130 frequency dependencies of saccadic suppression in primates[3,6,10].

131 To ensure that stimulus parameters were well matched with the RGC receptive field properties of
132 zebrafish, we additionally characterized receptive field sizes, response latencies and response polarities
133 of individual RGCs (Fig. 2). Adult zebrafish RGCs had receptive field sizes of 21.1 ± 6.6° (mean ± SD, n
134 = 87) (Fig. 2a). The coarse and fine textures used in this experiment had blob sizes of approximately
135 14.3° and 3.6° respectively (Methods), falling within the range resolvable by RGCs. With whole-field

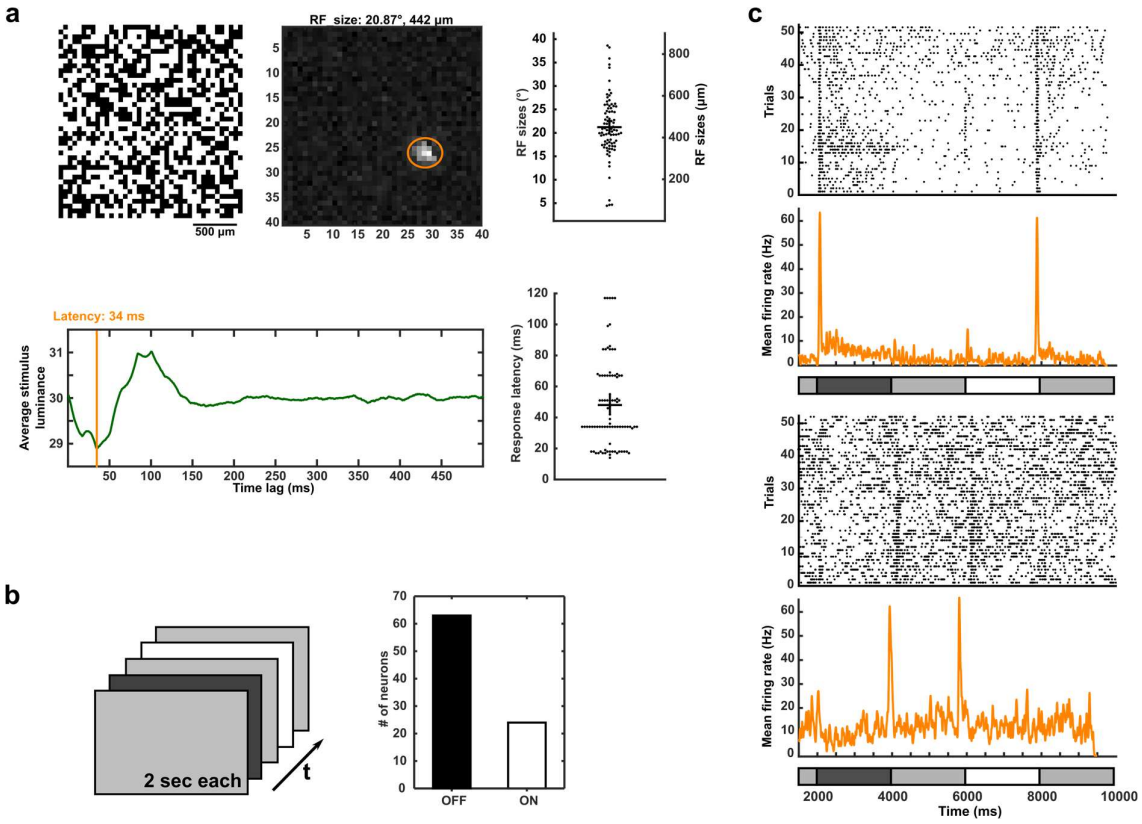

Fig. 2. Receptive field properties of zebrafish RGCs. a. Receptive field sizes and response latencies were characterized using a binary checkerboard flicker with a checker size of 55 x 55 µm. Orange ellipse indicates receptive filed size and orange line indicates response latency of an example RGCs, both determined as described in Methods. Group data (right panels) shows receptive filed sizes and response latencies of all RGCs recorded, error bars indicating mean ± SD. *N = 87 RGCs*. **b.** Whole-field contrast steps, each lasting 2 seconds were used to determine preferred polarity of RGCs. A majority of RGCs preferred light-to-dark (OFF) contrast steps over dark-to-light (ON) contrast steps. **c.** Spike count for individual trials and mean firing rate across trials during whole-field contrast steps for one example OFF RGC (upper panels) and one example ON RGC (lower panels).

contrast steps, preferred polarity of RGC responses was determined (Fig. 2b, c). Most RCGs were characterized as OFF cells and preferred a bright-to-dark contrast step (72.4%, 63/87 RGCs). Fewer RGCs were characterized as ON cells (27.6%, 24/87 RGCs). For the texture displacement experiment, RGCs were only analyzed for their preferred flash polarity; ON cells for bright flashes and OFF cells for dark flashes.

151 In summary, we showed with visual stimuli adapted to the visual acuity of zebrafish, that zebrafish
152 retinae modulate visual responses around the time of a saccade-like texture displacements with similar
153 temporal dynamics as mammalian retinae. While suppression strength is reduced, compared to
154 mammals, spatial frequency dependencies remain intact.

155

156 **Tectal neurons respond to dark flash stimuli in a 360° surround arena**

157 The optic tectum is the major retinorecipient area in the zebrafish brain[9]. To investigate how the above-
158 described retina-modulated responses are further processed in higher visual processing areas, we used
159 two-photon calcium imaging to image large populations of tectal neurons in larval zebrafish. Due to the
160 extremely large visual field of zebrafish[26,27], it is vital to provide true whole-field visual stimulation, when
161 studying saccadic suppression. Our recently established visual stimulation setup allows for high-
162 resolution 360° whole-field visual stimulation during calcium imaging (Fig. 3a). This enables us to
163 investigate the consequences of saccade-like texture displacements, analog to the retinal experiments at
164 the next step of visual processing. Tethered animals were again presented with global coarse and fine
165 textures. Textures were displaced horizontally in a saccade-like manner and at various delay times a
166 probe flash was shown. Probe flash parameters were slightly adjusted, to optimize for calcium imaging
167 in the OT (Fig. 3b). The duration of the flash was extended to 500 ms to allow for the relatively slow
168 calcium signal to integrate and only dark flashes were presented, since our own observations showed
169 that most OT neurons preferred dark stimuli over bright. Calcium recordings were registered and
170 segmented into individual ROIs, each representing one neuron (Methods). For each ROI, $\Delta F/F$ was
171 computed and regression-based analysis revealed many ROIs (14.9%, 12,397/83,104 ROIs) showing
172 significant responses to the flash stimulus (Fig. 3c). These responses are truly stimulus-associated, as

comparison with time-permuted traces showed (Fig. 3d), thus further allowing us to investigate how these visual responses are modulated by a texture displacement.

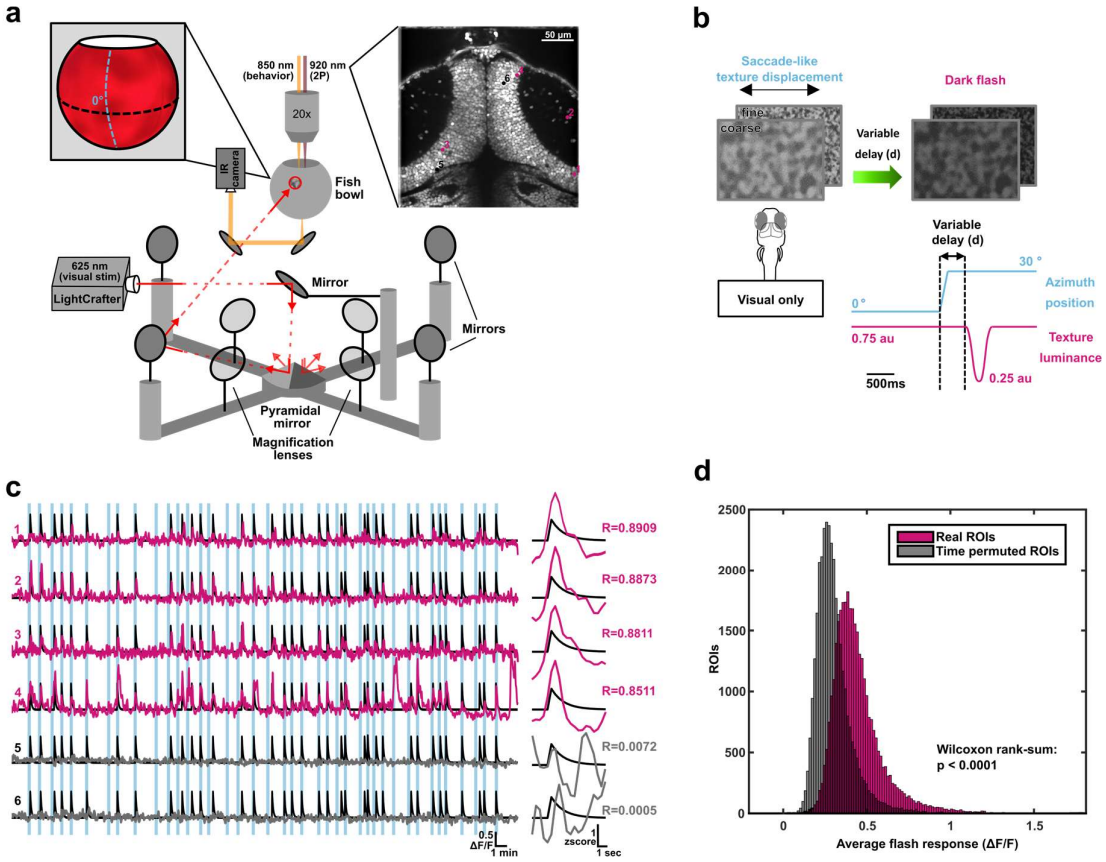

Fig. 3. Novel visual stimulation paradigm to study saccadic suppression in zebrafish optic tectum. a. Visual stimulation setup allows for whole-field visual stimulation onto a spherical projection surface, which encloses a live and behaving zebrafish larva (see left inset for photo of visual stimulus projected onto fish bowl). During visual stimulation eye position can be tracked using an infrared camera and activity of tectal neurons can be measured using 2P-imaging (right inset). Stimulus light was split by pyramidal mirror into four optical paths projecting onto the fish bowl screen surface **b.** Coarse and fine textures were displaced in azimuth on the spherical projection screen in a saccade-like manner. After a variable delay period (d), a dark probe flash was shown by reducing texture luminance. **c.** Regression-based analysis of fluorescence time traces of individual ROIs (each representing one tectal neuron) revealed many neurons responding significantly to the dark probe flash, while some neurons did not respond to the dark flash. The left panel shows ΔF/F traces of example neurons from the tectal slice shown in (a), across the entire recording; the right panel shows *z*-scores of responses to a flash shown in isolation for the same ROIs. Black lines indicate the stimulus regressor, blue bars indicate the time points of texture displacements and pink and gray traces indicate neuronal activity. Pink ROIs correspond to neurons with strong correlation coefficient, R to the stimulus regressor, gray ROIs represent neurons without strongly correlated responses to the visual stimulus. **d.** Average flash responses of all real ROIs recorded are larger compared to simulated ROIs with responses that were circularly permuted in time ($p < 0.0001$, two-tailed Wilcoxon rank-sum test, *n = 83,104 ROIs*).

193

194 **Texture displacement suppresses visual responses to global dark flash in the optic tectum**

195 To investigate how texture displacements modulate visual responses in the OT, we normalized flash
196 responses around the time of saccade to each ROI's response to a flash shown in temporal isolation.
197 Analogous to our analysis in zebrafish retinae, any responses associated to the texture displacement
198 were removed and remaining flash responses were quantified. When looking at all flash-responding
199 ROIs, we can see that more than 70% of neurons showed overall responses that were modulated
200 downward, thus suppressed, by the presence of a texture displacement (Fig. 4a, Supplementary Fig. 1a).
201 When comparing the 20% most suppressed and most enhanced cells to the same dataset with shuffled
202 delay identities, we can see that, not only are responses more suppressed in the real data (more green in
203 Fig. 4b, left), but enhancement is much weaker in the real data than expected by chance (less orange in
204 Fig. 4b, left).

205 We next tested whether the temporal profile of saccadic suppression is simply inherited from the retina
206 or does change in the tectum. From Fig. 4b it is apparent that most of the suppressed neurons have their
207 strongest suppression at 1000 ms or later after texture displacement onset (Fig. 4b, red box). This was
208 quite surprising to us as retinal suppression usually ends before 1000 ms (~250 ms in our dataset).
209 Texture displacements seem to modulate visual responses in the OT in a less straightforward fashion
210 than in the retina. This can not only be seen by this very late suppression in Fig. 4b, but also when
211 looking at the whole population of visual neurons in the OT. While there are, as previously stated, much
212 more suppressed than enhanced neurons, a spectrum of modulation exists, with many neurons also
213 being enhanced or not modulated at all (Supplementary Fig. 1a). Further, modulated neurons can be
214 found in the tectum in a more posterior-dorsal location, compared to all neurons registered in the
215 recording window ($p<0.0001$). This location corresponds to upper temporal visual space. The recording

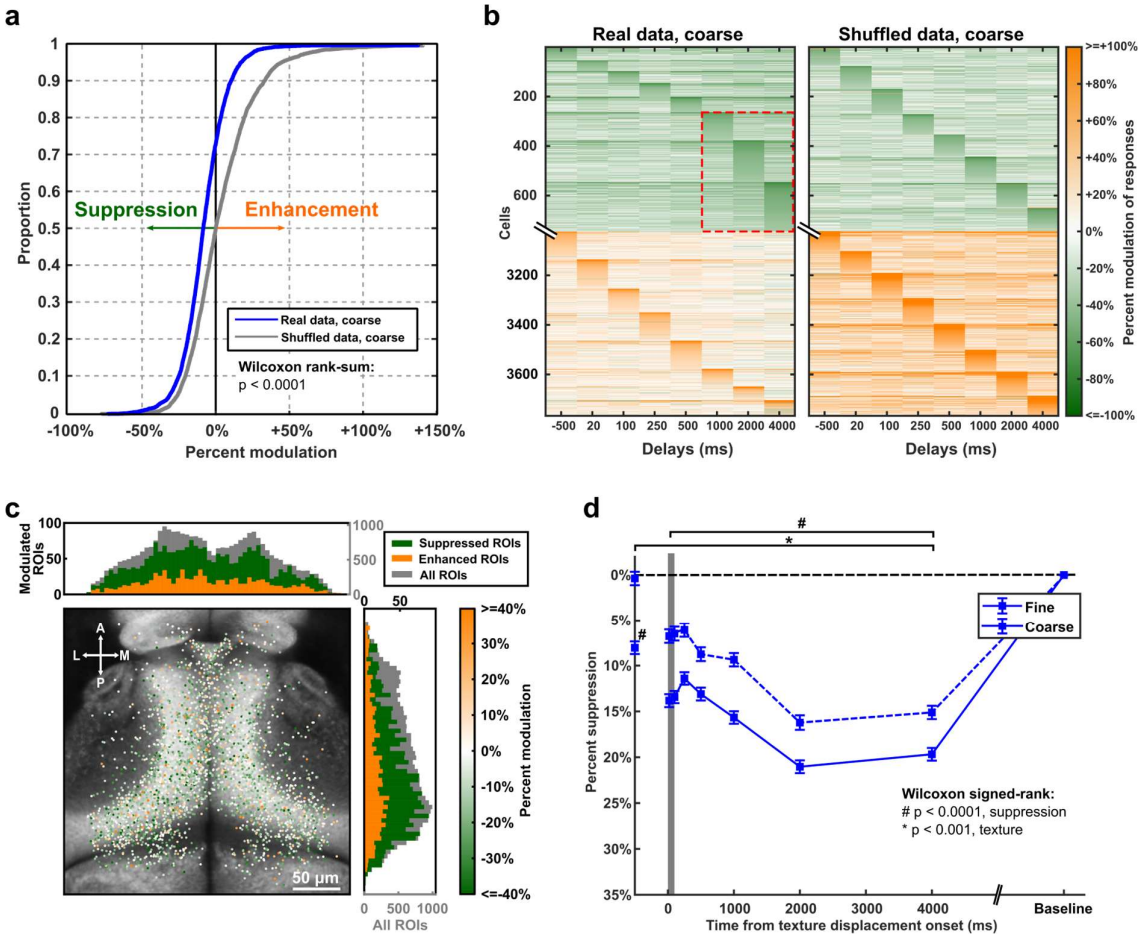

Fig. 4. Prolonged suppression in the OT after texture displacement. a. Cumulative distribution of flash response suppression across all flash-responsive neurons. Neurons were suppressed (or enhanced) by displacement of the coarse texture in a saccade-like manner (all delay times pooled). The majority of neurons have suppressed flash responses (curve for real data is shifted to the left relative to the curve for data with shuffled delay identities, $p < 0.0001$, two-tailed Wilcoxon rank-sum test, *n = 3,758 ROIs*). **b.** Modulation of flash responses at various flash delays of the 20% most suppressed and 20% most enhanced ROIs. Real data (left panel) shows stronger suppression and much weaker enhancement, compared to shuffled data (right panel). Red dashed box indicates that most of the suppressed neurons have their strongest suppression for delays ≥ 1000 ms. On the y-axis cells are sorted according strength of suppression/enhancement, peak delay time, and response magnitude at peak delay (for details see suppl. Fig. 1 and methods description). **c.** Center positions of all flash-responsive ROIs. Modulated ROIs can be found more posteriorly, compared to all registered ROIs ($p < 0.0001$ for enhanced vs. all ROIs and suppressed vs. all ROIs on AP-axis, two-tailed Wilcoxon rank-sum test, Bonferroni corrected, n = 866 enhanced ROIs, 2,330 suppressed ROIs, 31,944 total registered ROIs). There was no difference in anatomical distribution between enhanced and suppressed ROIs ($p = 0.18$ for enhanced vs. suppressed on AP-axis, $p = 0.78$ for enhanced vs. suppressed on ML-axis, two-tailed Wilcoxon rank-sum test, Bonferroni corrected). **d.** Dependence of percent suppression (mean ± SEM) on delay time for all suppressed neurons. Flash responses were significantly suppressed where indicated by a hash symbol (# $p < 0.0001$, two-tailed Wilcoxon signed-rank test, Bonferroni corrected for n = 24 conditions). Suppression was significantly stronger for coarse textures, than fine (solid vs. dashed line) for all delay times (* $p < 0.001$, two-tailed Wilcoxon signed-rank test). *N = 869 ROIs from 6 animals.*

window expanded to parts of the dorsal pretectum, where the proportion of modulated neurons was smaller, compared to the tectum (Supplementary Fig. 2). However, there was no difference in anatomical distribution between enhanced and suppressed neurons (Fig. 4c, Supplementary Fig. 2). To further investigate the temporal dynamics of saccadic modulation in the OT of not all, but only suppressed neurons, we used a permutation test to identify truly suppressed neurons independent of their actual temporal dynamics (Methods, Supplementary Fig. 3). Of the flash-responsive neurons 23.1 % (869/3758) were significantly suppressed and these neurons do in fact appear to inherit retinal suppression for delays up to 500 ms: Peak suppression for coarse and fine texture before 500 ms is nearly identical to retinal suppression (Fig. 4d, compare to Fig. 1e), with 13.8 ± 0.7% suppression for coarse and 6.8 ± 0.7% suppression for fine textures in the OT, compared to 15.8 ± 3.0% and 8.6 ± 3.4% in retina (mean ± SEM for all). The spatial frequency dependency observed in the retina remains intact as well. However, at delays ≥500 ms from texture displacement onset, a secondary, much stronger suppression occurs, with its peak at 2000 ms and 21.0 ± 0.7% (mean ± SEM) suppression of visual responses for coarse texture displacements.

We were startled by this finding, since saccadic suppression lasting >1 second in an ecological sense, would be quite a devastating loss of visual information. One possible explanation could be that our experiment did not truly assess saccadic suppression, but rather texture displacement suppression. In this paradigm the tectum only received visual information about an apparent saccade. It is, however, known in primates, that saccadic suppression is shorter with real saccades compared to visually simulated saccades[6,20]. This is why we investigated in our next steps, if the presence of a motor signal could shorten tectal suppression to values similar to other species. After all, in ecological settings, both visual and motor signals are present to shape saccadic suppression.

Motor signals strengthen early saccadic suppression, but do not abolish late suppression

Surprised by the exceptionally strong and long lasting extra-retinal suppression we observed in flash responses of tectal neurons following a visually simulated saccade, we tested if the presence of a motor signal could shorten saccadic suppression to an ecologically reasonable length. For this purpose, we had fish perform spontaneous horizontal saccades, either in front of a textured or uniform background. Saccades were detected online and again at various delay times after the saccade onset a global dark flash was presented (Fig. 5a, b). With the same regression-based analysis described above, visually responsive ROIs were identified and analyzed for their flash responses (Fig. 5b).

Once again, visual responses are diversely modulated up or down (Supplementary Fig. 1b). When looking at the 20% most suppressed neurons, it can be seen that the temporal suppression profile is much more structured than would be expected by chance (compare Fig. 5c and d, left with Fig. 5d, right), with and without visual feedback. Consistent with our findings in simulated saccades, more neurons are suppressed than enhanced (Supplementary Fig. 1b). With visual feedback, similar to the texture displacement experiment, more than 70% of neurons are suppressed across all delay times. Without visual feedback ~60% of neurons are still modulated downwards by a saccade (Fig. 5e), albeit less than with visual feedback. Therefore, suppression in the OT can also be mediated by a real saccade.

The visually induced saccadic suppression, which can be seen in texture displacement experiments in retina and OT is further altered in the presence of a motor signal. Peak suppression for early delays <500 ms is nearly doubled with a motor signal (13.8 ± 0.7% suppression for texture displacement vs. 26.4 ± 1.1% suppression saccade (mean ± SEM for both, coarse stimulus condition)). Further, we had anticipated that through the presence of a motor signal, long-lasting suppression after >500 ms would be weakened or even abolished. To our surprise, when looking at suppressed neurons, we could still see strong suppression multiple seconds after saccade onset (Fig. 5f). This time course of saccadic

suppression was also not altered by visual feedback. When saccades were made across a uniform background, we saw the same suppression strength and length as with a textured background. Therefore, saccadic suppression in the OT can be accomplished by motor signals alone in absence of visual feedback. This suppression is stronger than visual suppression alone, showing the strong influence of a corollary discharge signal in saccadic suppression.

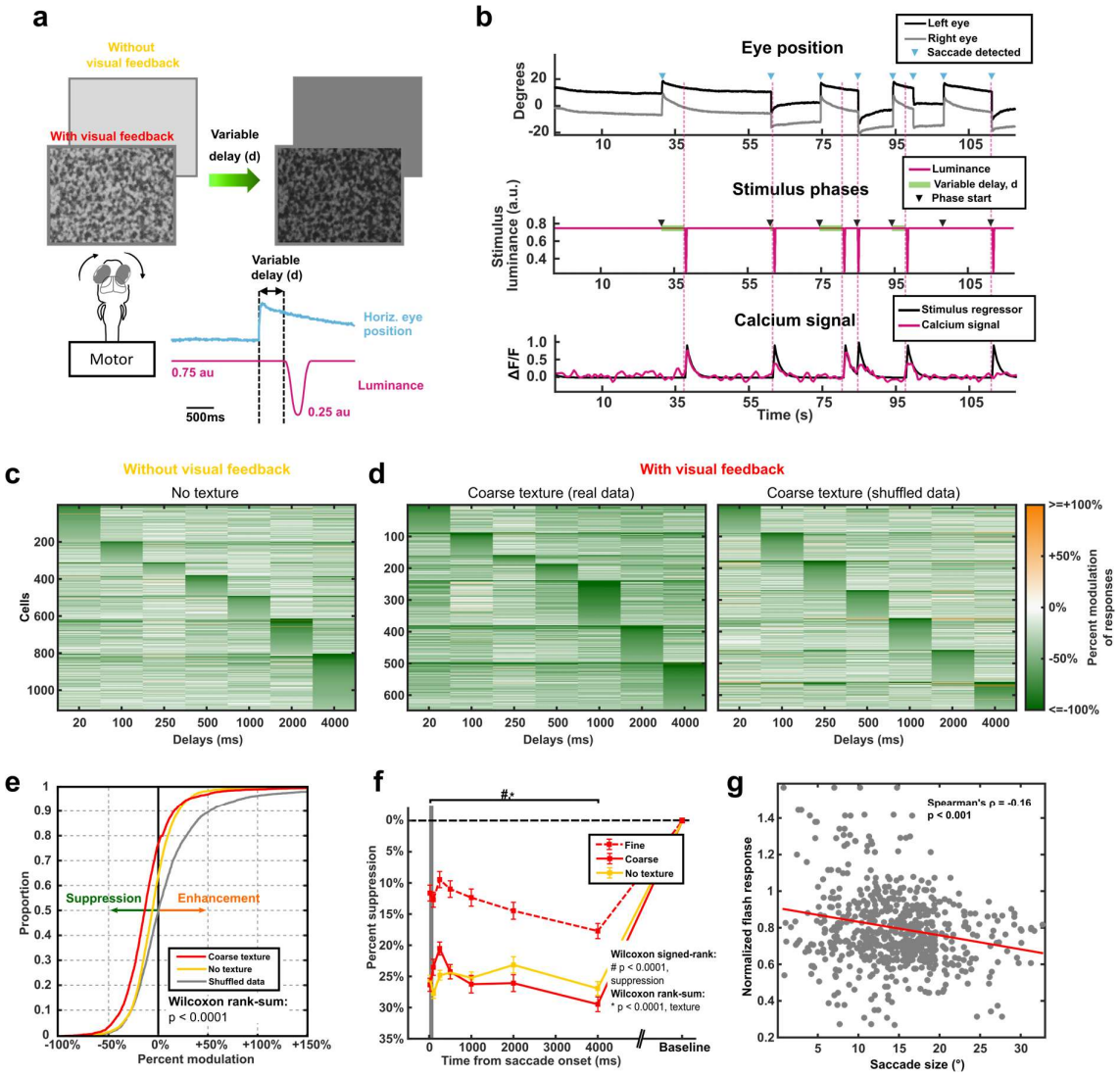

Fig. 5. Motor signals induce strong and long-lasting tectal saccadic suppression. a. Schematic of experimental paradigm. Fish performed spontaneous saccades either in front of a textured or uniform background. Saccades were detected online (blue trace) and after a variable delay period (d) a dark probe flash was shown, by reducing luminance of the texture or uniform background (pink line). **b.** Sample recording of closed-loop stimulus design. Eye position is tracked via IR camera and saccades are detected online (upper panel). Stimulus luminance is reduced after delay period (middle panel). An example neuron responds with a weaker ΔF/F signal for shorter delay periods, than for longer delay periods (lower panel). **c. & d.** Saccade-induced modulation of flash responses at various flash delays of the 20% most suppressed ROIs, without visual feedback (uniform background, panel c) and with visual feedback (textured background, panel d left). Temporal suppression profiles are more structured than expected by chance (shuffled data, panel d right). **e.** Cumulative distribution of saccade-induced modulation of flash responses in visual neurons across all flash delay times. A majority of visual neurons showed suppressed flash responses after a saccade across a coarse texture or across a uniform background; more than expected by chance ($p < 0.0001$, two-tailed Wilcoxon rank-sum test, n = 3,242 ROIs for textured background and shuffled data, 5,397 ROIs for uniform background). **f.** Temporal profiles of percent suppression of response (mean ± SEM) for all neurons suppressed by a saccade across coarse, fine or uniform background. Flash responses were significantly suppressed for all delay times and all backgrounds (# $p < 0.0001$, two-tailed Wilcoxon signed-rank test). Suppression was significantly stronger for coarse than fine textures (solid vs. dashed red line) for all delay times (* $p < 0.001$, two-tailed Wilcoxon signed-rank test). *N = 664 ROIs from 6 animals for textured background, n = 540 ROIs from 6 animals for uniform background.* **g.** Normalized flash response for delay times smaller than 500 ms and saccade size are negatively correlated, where larger saccades lead to more strongly suppressed flash responses ($p < 0.001$, Spearman rank correlation, n = 657 saccades).

If the purpose of such a corollary discharge signal is to act as a suppressive command for visual neurons during rapid eye movements, larger saccades, that lead to larger visual transient, should induce stronger suppression. Therefore, we tested if motor driven saccadic suppression in the OT might also correlate with saccade size. Particularly for early delay times <500 ms, where motoric suppression has its greatest effect, saccade size is indeed negatively correlated with normalized flash response, thus for greater saccade sizes, responses are down-modulated more strongly or suppressed (Fig. 5g), not however for late delay times ≥500 ms (Supplementary Fig. 4). This is in congruence with recent findings of a corollary discharge signal of saccade-like swim bouts in the zebrafish OT, which in size is positively correlated with swim vigor[21].

In summary, visual responses to global flashes are further modulated in the OT by the presence of a motor signal. Early saccadic suppression is stronger in the presence of a motor signal. In fact, motor signals alone, in the absence of visual feedback can elicit this suppression. Suppression strength is

correlated with saccade size, indicating that a corollary discharge signal is graded to the expected sensory signal that is to be suppressed. And lastly, both simulated and real saccades induce long lasting (>500 ms) suppression for global flash stimuli.

Saliency filtering can explain long lasting suppression in OT

After having found that motor signals can enhance early saccadic suppression but cannot abolish long-lasting suppression to a global flash stimulus, we considered the behavioral context of saccades in larval zebrafish. Larval zebrafish will perform non-reflexive saccades primarily to reorient their gaze and examine different parts of the visual field or in the context of prey capture to locate prey objects on the area centralis[15,28]. In both cases, it is beneficial for the animal to focus visual attention to local stimuli, such as an approaching predator or a small prey object. Now, if the animal was visually inhibited, due to saccadic suppression lasting several seconds past an actual saccade, behaviorally highly salient stimuli like predator and prey, could not be detected. Therefore, we suspected that late suppression, lasting >1000 ms could act like a visual saliency filter, ensuring efficient sensory processing, rather than saccadic suppression per se. While behaviorally relevant local stimuli could remain fully visible, less relevant global stimuli are suppressed.

To test this hypothesis, we combined a texture displacement with a local prey-like moving dot, rather than a global flash, as in previous experiments (Fig. 6a). The local dot stimulus elicited visual responses in fewer and more anterior-medially localized neurons, as is expected, due to the tectum's retinotopy[29] (Fig. 6b, corresponding to stimulus positions in the upper-nasal visual field). The responding neurons, however, had comparable response levels as those responsive to global flash stimuli in the previous experiments (Supplementary Fig. 5). As expected, visual responses were barely modulated across all

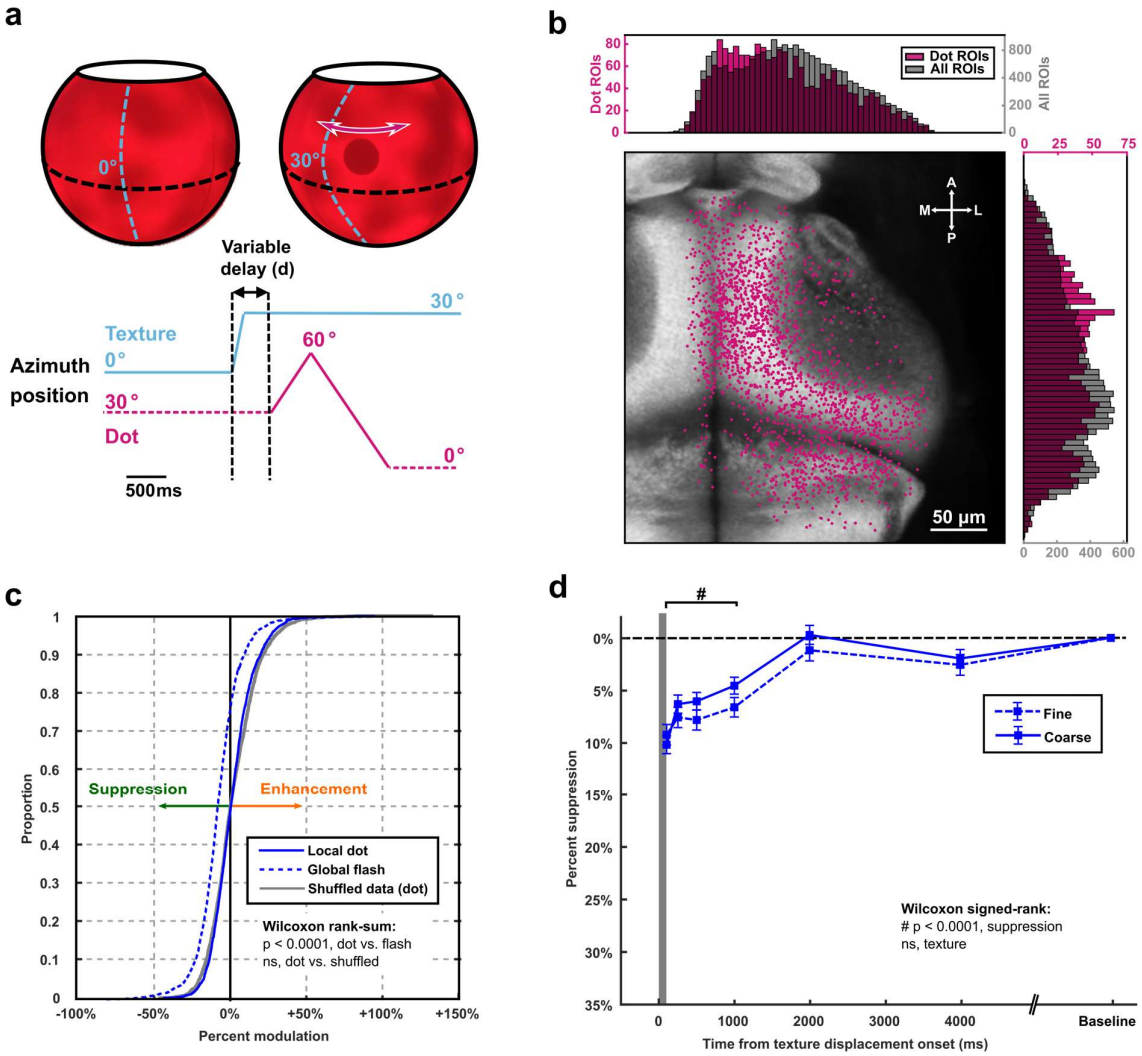

Fig. 6. Responses to local stimuli persist after simulated saccades. a. Texture displacement was paired with a local prey-like moving dot stimulus as a probe stimulus. Coarse texture was displaced in a saccade-like manner (blue line) and after a variable delay period (d) a dark dot with a diameter of 20° was shown at 10° elevation, moving in azimuth at 60°/s across the left frontal visual field (pink line, Methods). **b.** Center positions of ROIs that showed responses to the moving dot stimulus. Moving dot-responsive ROIs (pink) were located more medially and more anteriorly, compared to all ROIs (grey) that could be segmented within the recording window ($p < 0.0001$ for ML-axis, $p < 0.0001$ for AP-axis, two-tailed Wilcoxon rank-sum test, Bonferroni corrected, n = 2,048 dot-responsive ROIs, 18,497 total registered ROIs) **c.** Cumulative distribution of texture displacement-induced modulation of moving dot responses in visual neurons across all flash delay times. Unlike in experiments with a global flash probe stimulus (dashed blue line), for the local dot stimulus (solid blue line), visual neurons showed equal amounts of suppressed and enhanced responses following texture displacement as expected by chance ($p < 0.0001$ for local dot vs. global flash, $p > 0.05$ for local dot vs. shuffled data, two-tailed Wilcoxon rank-sum test, n = 2,259 ROIs) **d.** Temporal profile of response suppression for local dots (mean ± SEM) for all neurons suppressed by a displacement of a coarse or fine texture. Local dot responses are only suppressed for delay times ≤1000ms for both coarse and fine textures (# $p < 0.0001$, two-tailed Wilcoxon signed-rank test). There was no difference between the two textures ($p > 0.05$, two-tailed Wilcoxon signed-rank test). *N = 504 ROIs from 3 animals.*

364 delay times, and we did not see more suppressed than enhanced neurons, like we did in previous global
365 flash experiments (Fig. 6c). When looking at truly suppressed neurons only, we can see that there is only
366 very weak suppression for early delay times; late suppression is completely abolished (Fig. 6d). This
367 early suppression is likely inherited directly from the retina, as it follows a roughly similar time course
368 and suppression strength (compare two black lines in Fig. 7a).

369 Overall, we show that late saccadic suppression lasting >1000 ms is heavily dependent on the probe
370 stimulus used. While global stimuli, such as a global flash, remain suppressed for several seconds after
371 a saccade, behaviorally relevant local stimuli, such as a prey-like dot, become quickly perceivable again.
372 This task-specific processing of visual information in the tectum could function as a saliency filter,
373 ensuring efficient sensory encoding for zebrafish that have limited neural capacities.

374

375 **Saccadic suppression is shaped by the type of visual stimuli and motor signals in zebrafish OT**

376 When combining the observations from all experiments described above, we can identify both visual
377 and motor-related mechanisms that shape saccadic suppression dynamics across the zebrafish visual
378 system (Fig. 7a, Fig. 8). In isolated adult retinae, RGC responses to global flash stimuli are weakly
379 suppressed for up to 250 ms; the suppressed signal is relayed to the OT. Here, visual responses of larval
380 tectal neurons are even more strongly suppressed by a real saccade, than a simulated saccade,
381 particularly in the first 500 ms after saccade onset. At later time points (≥1000 ms) after saccade onset,
382 global and local visual stimuli are differentially processed by tectal neurons. While responses to global
383 flashes are strongly suppressed for several seconds, responses to a local prey-like dot, after weak early
384 suppression in the first 1000 ms after saccade onset, quickly return to baseline response level.

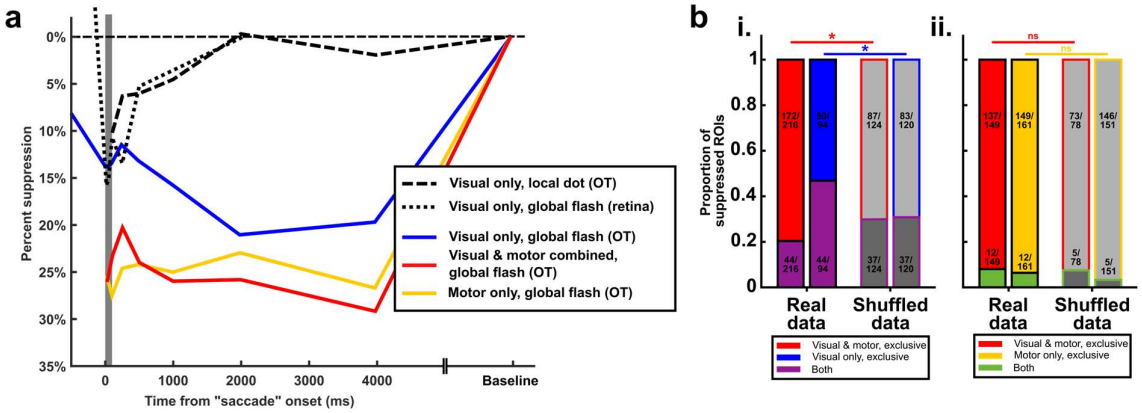

Fig. 7. Visual and motor signals act on non-overlapping neural populations in the OT. a. Temporal suppression profiles in retina and OT of all visual and motor conditions tested in this study. Visual Only refers to experiments with simulated saccades on a textured background, Visual & Motor Combined refers to experiments with real saccades across a textured background, and Motor Only refers to experiments with real saccades across a uniform background. **b. i.** Proportions of neurons suppressed exclusively in the Visual & Motor Combined condition (red) or exclusively in the Visual Only condition (blue) versus neurons suppressed in both conditions (purple) when tested within the same animal, compared to the proportions in data with shuffled condition identities. There are more Visual & Motor, exclusive suppressed neurons than expected by chance ($p < 0.05$, χ^2-test for proportions) and less Visual Only, exclusive suppressed neurons than expected by chance ($p < 0.05$, χ^2-test for proportions). **ii.** Proportions of neurons suppressed exclusively in the Visual & Motor Combined condition (red) or exclusively in the Motor Only condition (yellow) versus neurons suppressed in both conditions (green) when tested within the same animal, compared to the proportions in data with shuffled condition identities. Only few neurons are suppressed in both conditions, no more than expected by chance ($p = 0.27$, χ^2-test for proportions), suggesting that they are separate populations.

Lastly, when investigating motor and visual effects in neurons of the same animal, we found non-overlapping populations of neurons. While some neurons were exclusively suppressed through the visual feedback of a texture displacement (50/94 ROIs, 53.2%), a large proportion of those suppressed through texture displacement could also be suppressed through a saccade across texture (44/94 ROIs, 46.8%), more than would be expected by chance (Fig. 7b, i.). However, most of the neurons, that were suppressed through a real saccade, were not suppressed in the simulated condition (172/216 ROIs, 79.6%), indicating that those neurons required both motor and visual feedback; visual feedback alone did not suffice. When comparing saccades with visual feedback to saccades without visual feedback in

411 neurons of the same animal, we found that almost all neurons are exclusively suppressed in either one
412 of the two cases, saccades with visual feedback (137/149 ROIs, 91.9%) or saccades without visual
413 feedback (149/161 ROIs, 92.5%). Very few neurons are suppressed for both, no more than expected by
414 chance (Fig. 7b., ii.), indicating that this could be two separate populations of neurons.

415

416 **Discussion**

417 We identified distinct visual and motor-related processes, shaping saccadic suppression on a neuronal
418 level across the zebrafish visual system (Fig. 8). Purely visual effects, such as masking, already take place
419 in the zebrafish retina prior to entering the OT. Following a saccade-like texture displacement, RGCs
420 show suppressed responses to peri-saccadic visual stimuli. The length of the peri-saccadic suppression
421 window in zebrafish retina is comparable to that found in mammals, but suppression strength is much
422 weaker[6]. Spatial frequency dependencies of suppression are similar to those observed in mammals in
423 that low spatial frequency content is more strongly suppressed than high spatial frequency content.
424 Zebrafish have lower visual acuity though, so the stimuli were coarser in this study than in research on
425 mammals.

426 This modulated retinal signal gets further relayed to the OT, the major retinorecipient area in the
427 zebrafish brain. There, saccadic suppression is further shaped by both visual and motor signals. Saccade-
428 like texture displacements elicit saccadic suppression of visual responses in the OT just as in the retina.
429 In fact, suppression in the early peri-saccadic window (delays <500 ms) is likely directly inherited from
430 the retina, as it follows the same time course and has nearly identical suppression strength. When
431 comparing purely visually induced "saccadic" suppression to saccadic suppression following an actual
432 spontaneous saccade, we found that the execution of an actual motor command significantly increases

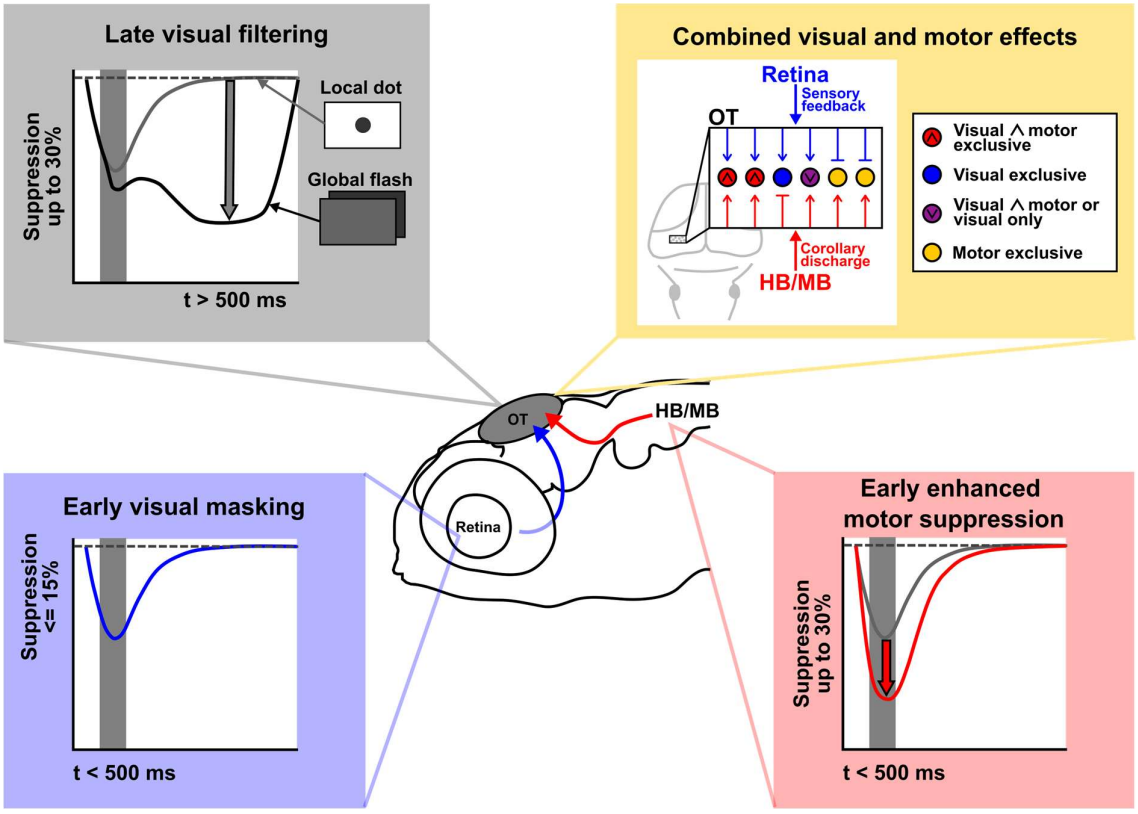

Fig. 8. Visual and motor mechanisms shape saccadic suppression throughout the zebrafish visual system. Both visual and motor-related signals shape the temporal profile of saccadic suppression in the zebrafish. Purely visual mechanisms (i.e. visual masking) lead to early, weak saccadic suppression in the retina (blue box). Retinal signals are sent to the OT and further modulated. Motor signals, likely originating from the hindbrain oculomotor circuits, strengthen early saccadic suppression in the OT (red box). Visual filtering mechanism in the OT can alter late saccadic suppression to last more than 1000 ms (gray box). Behaviorally salient stimuli, such as a local dot, are not further suppressed, whereas behaviorally irrelevant stimuli, such as a global flash are suppressed for long time scales (gray box). Motor and visual signals act together on different types of tectal neurons. While some neurons are only suppressed by either a visual or a motor signal, most neurons integrate suppression from both signals (yellow box).

suppression strength in the early peri-saccadic window. This result suggests that corollary discharge signals play an important role in strengthening saccadic suppression. The observed saccade-size dependency (Fig. 5g) supports this idea. Corollary discharge signals are known to play a vital role in optimizing sensory processing during self-motion across the animal kingdom[30–32] and recently, it has been shown that the zebrafish OT receives corollary discharge signals during saccade-like swim bouts[21].

451 It is likely that eye movement signals could elicit a similar corollary discharge signal in zebrafish, and
452 our observed "motor only" saccadic suppression with a homogeneous visual background suggests that
453 these corollary discharge signals exist. Future studies are needed to measure the saccadic corollary
454 discharge signal more directly in the zebrafish OT and demonstrate its mechanistic involvement in
455 saccadic suppression.

456 On a behavioral level, in primates, motor signals are known to shorten the peri-saccadic suppression
457 window[33], potentially due to post-saccadic excitability enhancement in cortical areas[34–36]. The lack of a
458 cortex is thus a potential proximal explanation for the lack of a motor-associated temporal restriction
459 of saccadic suppression in zebrafish.

460 Another striking difference between saccadic suppression in the zebrafish OT and saccadic suppression
461 in primates is a strong secondary suppression in zebrafish, particularly of global flash responses for
462 several seconds past the saccade onset. This was true for simulated saccades and real saccades with and
463 without visual feedback. We were struck by this finding, as from an ecological perspective, it seems like
464 a massive loss of visual information, to discard sensory signals for up to 4 seconds after a saccade. Using
465 an imaging technique with very slow temporal resolution of ~2 Hz, attempting to resolve an effect that
466 ought to play in the tens and hundreds of millisecond time scale, we were concerned that the slow
467 suppression dynamics were an artifact of our stimulus design and poor temporal resolution. Thus, in a
468 small subset of recordings, we tested a short 20 ms flash stimulus, comparable to the brief probe flash
469 used in the high temporal resolution MEA recordings in the retina. In order to capture small and rapidly
470 changing neural responses to this brief visual stimulus, we chose to image a much smaller brain region,
471 but at 50 fps temporal resolution. We found that even with this brief visual stimulus, and with
472 recordings at high temporal resolution, suppression lasting >1000 ms remained (Supplementary Fig. 6).

473 We propose that the persistent suppression is a task-specific efficient encoding strategy for the larval
474 zebrafish, which has to deal with limited neuronal resources. Since spontaneous saccades are often
475 followed by the detection of a local visual stimulus, either in a prey capture setting or when detecting a
476 predator[15,28], it would be sensible for the fish to focus its neural resources to accurately detecting local
477 visual stimuli and discarding information about global stimuli. This is exactly what we found when
478 testing a local prey-like dot stimulus for saccadic suppression in the OT. While the visual suppression
479 inherited from the retina remains intact, there is no further modulation of the visual signal after the
480 initial peri-saccadic window. Such attentional filtering for behaviorally salient stimuli following a
481 saccade has already been predicted in computational models of cortical population activity; in a
482 competitive interaction between two stimuli, modeling studies predict suppression of unattended
483 stimuli to enhance sensitivity to relevant stimuli[37]. Further, studies in archerfish have shown that the
484 teleost optic tectum is capable of using visually driven long-range inhibition, i.e. inhibition modulated
485 by signals from outside the receptive field, to aid in selecting behaviorally salient stimuli, such as prey
486 over behaviorally irrelevant stimuli[38]. In the archerfish retina, saccades might serve to encode visual
487 stimuli with higher fidelity[39]. Overall, future studies are needed to reveal the differential suppression of
488 various ecologically relevant visual stimuli in the context of saccadic suppression. In the cortical area
489 V1 of primates, preliminary data suggests that dark contrasts are not suppressed at all, unlike in superior
490 colliculus and primate perception[40,41], which could represent an ecological adaptation as well, and this
491 phenomenon needs to be addressed in comparative studies. Furthermore, a better understanding of the
492 receptive field properties and functional roles of tectal neurons will be required to fully understand why
493 and how different visual signals are suppressed in the OT.

494 Lastly, we investigated how visual and motor signals can act on tectal neurons within the same animal.
495 We have found that while there are many neurons that can be suppressed purely by a visual signal of a

simulated or real saccade across a texture, a larger proportion of neurons requires a simultaneous motor signal, arising from an actual saccade in order to be suppressed. Further, when comparing which neurons are suppressed through the execution of a saccade in the absence of any visual feedback to those suppressed through a saccade with visual feedback, we found that there is almost no overlap between these two cell populations. It is unclear why motor suppression and visually driven suppression are segregated in such a manner. It seems that saccadic suppression is used as a precise tool for various different contexts. This suppression layout across the neuronal population could be the results of balancing suppression against information loss, since only small populations are suppressed, and only under certain conditions.

In summary, we identified that saccadic suppression exists in the small-brained larval zebrafish, and that visual and motor signals play differential roles. Compared to mammals, zebrafish saccadic suppression is weaker but longer-lasting. Further studies are needed to reveal conserved mechanisms that govern saccadic suppression and potentially explain the observed differential expression of suppression dynamics across species.

Methods

Zebrafish

For retinal recordings we used retinae of *nacre* +/- adult zebrafish (*Danio rerio*), which are functionally wild type. Ten retinae from 6 male and 4 female fish (age 8-23 months) were used. Adult zebrafish were housed at our local animal facility at 28°C water temperature at a 14/10h light/dark cycle. Animals were brought to the laboratory space and dark-adapted for several hours prior to retinal tissue preparation.

517 For *in-vivo* calcium recordings, larval zebrafish, age 5-7 dpf, with pan-neuronal GCaMP6f expression
518 and homozygous for the *mitfa* mutation were used (*Tg(HuC:H2B-GCaMP6f)jf7; nacre -/-*)[42]. Zebrafish
519 were reared in E3 solution at 28°C on a 14/10 light/dark cycle. At 4 dpf, animals with the strongest GFP
520 expression were selected for subsequent recordings at 5-7 dpf. Animal experiments and all experimental
521 protocols were approved by the responsible ethics committee of the Regierungspräsidium Tübingen in
522 accordance with German federal law and Baden-Württemberg state law. All animal procedures also
523 conformed to the institutional guidelines of the University of Tübingen.

524

525 **Retinal electrophysiology**

526 **Tissue preparation (MEA).** Fish were dark adapted for a minimum of 2 hours, before they were killed
527 under dim red light either with anesthetic overdose (250 mg/L Tricaine, Pharmaq, in fish water) or
528 through rapid chilling (~2-4°C). Afterwards, animals were decapitated and the eyes were removed and
529 placed into chilled Ringer solution (in mM: 110 NaCl, 2.5 KCl, 1.0 CaCl2, 1.6 MgCl2, 10 D-Glucose,
530 and 22 NaHCO3) bubbled with 5% CO_2 and 95% O_2. Retina was isolated inside a Ringer bath, placed
531 into 5% Hyaluronidase solution for 3 min to remove remaining vitreous and then placed into warmed
532 Ringer solution (~30°C) for one hour to recover tissue. Following recovery, retina was mounted onto a
533 nitrocellulose filter (Millipore) with a central 1.5 x 1.5 mm hole and placed RGC side down onto a
534 perforated low-density multi-electrode array (60pMEA200/30iR-Ti-gr, Multichannel Systems,
535 Reutlingen, Germany) with 60 electrodes in a square-grid arrangement and 200 µm inter-electrode
536 distance. Good electrode contact was ensured through negative pressure through the perforation over
537 at least 30 minutes, prior to recording begin. Tissue was superfused with bubbled Ringer solution at
538 ~30-32°C. Data were acquired at 25 kHz using MC Rack version 4.6.2 (Multichannel Systems).

539

540 **Visual stimulation (MEA).** Visual stimuli were adapted from Idrees and colleagues[6]. A spectral
541 intensity profile (in μW cm^{-2} nm^{-1}) of the visual stimulus was measured with a calibrated USB2000+
542 spectrometer (OceanOptics, Orlando, FL, USA) and converted into biological units (R* rod^{-1} s^{-1})[43]
543 normalized zebrafish rod absorbance[44] (2.4 μm^2 for zebrafish rods[45]). On the DLP projector scale (0-
544 255) a stimulus intensity of "60" with ND5 filter (which was used in almost all retinal recordings)
545 equaled 3442 R* rod^{-1} s^{-1}.

546 Two binary Gaussian blur textures with differing spatial scales were used in the experiment. The fine
547 texture had image blobs with a size of 75 μm, the coarse texture had blobs of 300 μm. In adult zebrafish,
548 this equates to approximately 3.5° and 14.3° of retinal surface for fine and coarse texture respectively[46].
549 The pixel intensity of the textures ranged from 30-90 with a mean intensity of 60 on the 8-bit DLP
550 projector scale (0-255).

551 In order to simulate saccades, the texture was rapidly displaced for 100 ms at 100 to 300°/s at a straight
552 trajectory in random direction. At various time points around the texture displacement (-150, 17, 50,
553 100, 250, 500, and 2000 ms after texture displacement onset) a probe flash was shown. The probe flash
554 was a full-screen positive or negative luminance step ("bright" or "dark" flash), that lasted for one frame
555 (16.7 ms). Local contrast within the texture remained constant between the probe flash and the
556 background texture. In total a single trial consisted of 15 conditions (7 delays with dark flash, 7 delays
557 with bright flash, 1 control displacement without flash) shown in random order; trials were repeated at
558 least four times for each texture type. Additionally, the following stimuli were shown to characterize
559 RGCs types and receptive field properties: 1. Full field contrast steps. To test ON/OFF properties of
560 RCGs, uniform background luminance steps from 30 to 60 and from 60 to 90 pixel intensity steps in
561 positive (ON) and negative (OFF) direction were shown. 2. Binary checkerboard flicker. For spatial

562 receptive field mapping a binary checkerboard pattern, with checkers of 55 x 55 μm size, randomly
563 switching between 10 or 50 pixel intensity independent of other checkers was shown. The stimulus was
564 shown for 10 minutes. Linear filters, representing spatial and temporal receptive fields were calculated
565 through reverse correlation.

566

567 **Data analysis (MEA).** MEA recordings were high-pass filtered at a 500 Hz cutoff frequency using a
568 tenth-order Butterworth filter. Spikes were sorted semi-manually using Matlab-based custom software,
569 and spike waveforms and times were extracted according to Idrees and colleagues[6]. RGC types were
570 characterized based on their responses to full-field contrast steps. For each cell an ON/OFF index was
571 calculated by dividing differences between ON and OFF step peak response by their sum. The index
572 ranged from -1 to +1, where -1 indicates a full OFF cell and +1 indicates a full ON cell. Cells with an
573 ON/OFF index > 0 where only analyzed for bright probe flashes and cells with an ON/OFF index < 0
574 were only analyzed for dark probe flashes. Further, we characterized the spatial receptive field of each
575 cell, by examining the linear filters for each region (checker) defined by the binary checkerboard
576 stimulus. A 500 ms window prior to each spike was summed and the modulation strength of each linear
577 filter, measured as the standard deviation along the 500 ms kernel, determined how strongly that
578 checker drives the RGC. The resulting 2D map of standard deviation values was fitted with a 2D
579 Gaussian, and receptive field size was determined as an ellipse with 1.5σ. Receptive field sizes were
580 converted from x μm to α degrees approximating the focal length (f) of the adult zebrafish eye as
581 1.2mm[46], such that $\alpha = 2\tan^{-1}\left(\frac{x}{2f}\right)$. Response latency was determined as the time from stimulus onset
582 to 90% peak response. All spike times were converted into firing rates (spikes/s) by convolving spike
583 times with a Gaussian of σ = 10 ms standard deviation and amplitude $0.25\,\frac{\sqrt{e}}{\sigma}$.

584 To determine retinal saccadic suppression for each recorded RGC, first baseline responses were defined
585 as peak firing rates in response to probe flashes at 2000 ms delay from texture displacement onset,
586 averaged across trials. Then, average peak firing rates of the same RGC to all other delay times were
587 normalized to this baseline response. Any texture displacement related responses were identified in
588 control trials, without probe flashes and averaged across trials for coarse and fine textures
589 independently. Flash responses were isolated from texture displacement responses by subtracting
590 average texture displacement responses from the total responses, leaving only the flash-related response.

591

592 ***In-vivo* calcium imaging**

593 **Visual stimulation and recording setup.** All visual stimuli used in this study were displayed on a
594 custom-built spherical stimulation arena, with simultaneous eye position recordings. In the stimulation
595 arena, fish were placed inside a custom printed Ø 80 mm resin bowl (Accura ClearVue, SLA resin, 3D
596 Systems GmbH, Meorfelden-Walldorf, Germany), evenly coated in white acrylic spray paint and sealed
597 with clear varnish. The resin fish bowl served as a projection surface for a DMD video projector
598 (LightCrafter E4500 MKII, EKB Technologies Ltd., Israel), powered by a multispectral high power LED
599 light source (CHROLIS, 365/420/470/625 nm, Thorlabs GmbH, Bergkirchen, Germany). In order to
600 cover the entire projection surface of the bowl, the image of the video projector was split into four paths
601 by a pyramidal mirror and refocused onto the fish bowl from all four sides (Fig. 3a) to cover -90° to
602 +45° in elevation and 360° in azimuth. All stimuli were presented at 60 Hz refresh rate at 625 nm (red)
603 to avoid light interference with calcium imaging. Irradiance and corresponding Michelson contrast
604 inside the fishbowl were measured using an optical power meter (Newport 1918-R optical power meter
605 with 918D-SL-OD3R detector, Newport Corporation, Irvine, CA, USA) and a Ø 5 mm liquid core light
606 guide (Thorlabs GmbH, Bergkirchen, Germany) positioned on the inside wall of one half bowl at

607 various elevations. At 625 nm stimulation wavelength the following measurements for high irradiance,
608 low irradiance and Michelson contrast were made at 22.5°, -22.5°, and -77.5° elevation: 22.5°: 8.56
609 mW/m^2 high, 0.51 mW/m^2 low, 0.89 contrast; -22.5°: 17.83 mW/m^2 high, 0.61 mW/m^2 low, 0.93
610 contrast; -77.5°: 5.79 mW/m^2 high, 0.61 mW/m^2 low, 0.81 contrast.

611 A custom-built 850 nm IR-LED ring provided illumination for eye position tracking through the
612 excitation path. A small window in the spherical stimulation arena below the fish (~5 mm diameter)
613 allowed for recording of eye potion with an infrared-filtered camera at 100 Hz (Basler ace 2 R, a2A1920-
614 160umBAS, Basler AG, Ahrensburg, Germany).

615 *VxPy* (Version 0.1.4) was used to generate and display visual stimuli, as well as record eye position traces
616 and trigger visual stimuli in a closed-loop manner.

617

618 **Visual stimulation protocol (Calcium Imaging).** Visual stimuli were designed in analogy to retinal
619 stimulation, but adjusted to the geometry of our stimulation arena. Instead of using a rectangular array
620 of black and white pixels and convolving these with Gaussians, we designed a stimulus in spherical
621 coordinates by first placing equidistant nodes on the surface of a unit sphere. Half of the nodes were
622 randomly selected as "bright" nodes, and identical von-Mises-Fisher distributions with concentration,
623 $\kappa = 5.6$ were placed centered on each of these. Nothing was placed on the remaining, "dark" nodes. After
624 summing up all distributions, intensities were rescaled to impose a desired minimum and maximum
625 across the sphere surface to ensure roughly uniform local luminance and contrast across the visual field.
626 The number of nodes is the parameter that determines pairwise distances between them. Its values were
627 chosen to produce stimuli with spatial frequencies (Supplementary Fig. 7) that reliably elicit behavioral

628 responses. For the coarse texture 2,000 nodes (1,000 bright) were used, for the fine texture 4,000 nodes
629 (2,000 bright) were used.

630 In "texture displacement" experiments, saccades were simulated through a rapid rotation of the texture
631 on the vertical axis by 30° at 300°/s either to the left or right. In "real saccade" experiments, saccades
632 were detected with a velocity threshold of at least 200°/s. Saccade threshold was individually adjusted
633 for each fish, to ensure best saccade detection, without noise interference.

634 At various delay times around texture displacement onset or saccade detection a probe stimulus was
635 presented. Delay times were usually -500, 20, 100, 250, 500, 1000, 2000, and 4000 ms, unless stated
636 otherwise. In "real saccade" experiments, no pre-saccadic stimulus could be shown. Probe stimuli were
637 shown twice without texture displacement or 8 s after real saccade onset and used as baseline stimuli.
638 Additionally, texture displacement/saccade occurred without probe stimulus. Therefore, one trial
639 consisted of 9-11 conditions (6-8 delays, 2 baseline probes, 1 control displacement/saccade), shown in
640 random order; trials were repeated at least 4 times.

641 In flash experiments the secondary visual stimulus consisted of a whole-field luminance decrease with
642 a cosine shape, lasting 500 ms at 0.5 Hz and an amplitude of 50% luminance change. For high frequency
643 recordings, a luminance step, lasting 20 ms with an amplitude of 50% luminance decrease was used.

644 In moving dot experiments, a dark dot, moving across the static texture was used as a secondary visual
645 stimulus. The moving dot had a 20° diameter and was located in the upper left visual field at 10°
646 elevation. The dot moved at 60°/s in azimuth from -30° to -60° and back to 0° over a time span of 1.5 s.
647 To avoid movement overlap between the texture displacement (lasting 100 ms) and the moving dot
648 stimulus, only delay times ≥ 100 ms were used in the moving dot experiment.

649

650 **Two-photon calcium imaging.** For in-vivo calcium imaging, fish were embedded in 1.6% low-melting
651 agarose and placed onto a custom-built stage, which could be attached to a holder on the inside of the
652 spherical stimulation arena. For the stage, the tip of a plastic Pasteur pipette was cut and shaped into an
653 arrowhead shape. Then, the pipette tip was placed into a custom 3D-printed mold and 2.5% low-melting
654 agarose was poured into the mold resulting in a transparent stage that allowed the fish to be placed
655 central inside the spherical stimulation arena. For "real saccade" experiments, agarose was removed
656 around the eyes of the fish, to allow for free eye movements. Once the fish was placed in the center of
657 the spherical stimulation arena dorsal side up, it was filled with clear E3 medium. The position of the
658 fish could be adjusted, to correct for potential roll.

659 Calcium activity of tectal neurons was recorded with a movable objective two-photon setup (Sutter
660 Instruments, Novato, California, USA), previously described[47]. The calcium indicator was excited at 920
661 nm and emitted light was collected with a 20x/1.0 Zeiss objective. In most recordings image acquisition
662 rate was 2.18 fps, with 512 x 512 pixels imaged. Only in high-speed recordings a smaller window (40 x
663 40 pixels) was imaged at 50 fps acquisition rate. Magnification ranged from 1-2x, where 1x results in a
664 resolution of 0.88 µm x 0.88 µm per pixel.

665

666 **Data analysis (Calcium imaging).** Calcium recordings with 2.18 Hz acquisition rate were registered
667 and segmented with suite2p[48] into individual ROIs, each representing one tectal neuron. A time
668 constant of 1.61 s was used and for recordings at 1.6x magnification a cell diameter of 10 pixels (5.5 µm)
669 was used. For different magnifications, the cell size was adjusted accordingly. The suite2p built-in
670 selection algorithm *is-cell* was ignored. High-speed recordings with 50 fps acquisition rate were
671 segmented manually in Fiji (ImageJ) into elliptical ROIs, based on standard deviation projections.

672 Center positions of segmented ROIs were registered to the Max Planck Zebrafish Brain (mapzebrain)
673 atlas[49] using ANTsPy[50].

674 Further data analysis was performed using custom-written Matlab (The MathWorks Inc., Natick, USA)
675 and Python (PyCharm, JetBrains, Prague, Czech Republic) scripts. Fluorescence traces for each ROI
676 were normalized into $\Delta F/F_0$, with a sliding window median of 120 seconds for F_0. Through a regression-
677 based analysis, ROIs that responded to the secondary visual stimulus used in the experiment (flash or
678 moving dot), when shown in temporal isolation ("baseline", i.e. without saccade or texture
679 displacement), were identified and only those ROIs were considered for further analysis
680 (19,784/119,220 ROIs across all flash experiments, 16.6%, 2,210/20,789 ROIs for moving dot
681 experiment, 10.6%).

682 Saccade- and texture displacement-associated activity in ROIs was identified, by averaging calcium
683 traces during the saccade/texture displacement from control conditions (without secondary visual
684 stimulus) and long delay conditions (≥2000 ms) up to the point of secondary visual stimulus
685 presentation. Average saccade-/texture displacement-associated activity was then subtracted from the
686 calcium trace for the time points during and shortly after the saccade/texture displacement.

687 Peak $\Delta F/F$ responses to the secondary visual stimulus at each delay time were quantified and averaged
688 across trials for each ROI. For "real saccade" experiments, trials in which fish performed undesired
689 saccades between the initial saccade and presentation of the secondary visual stimulus were discarded.
690 Trials, in which the fish struggled, thus rapidly moved its head, rather than performing an actual saccade
691 were also discarded. Average peak $\Delta F/F$ responses were normalized to average baseline responses
692 without saccade/texture displacement. Individual modulation curves for each ROI were generated as in
693 Supplementary Fig. 2b.

694 To identify suppressed ROIs, amongst all ROIs sensitive to the visual stimulus, modulation curves of
695 individual ROIs were first correlated against 6-8 model suppression curves (Supplementary Fig. 2c),
696 depending on the number of delays used in the experiment. Model suppression curves had different
697 delay times of peak suppression and each a unimodal modulation. The average modulation across all
698 delays had to be <1, thus suppressed. Out of the model suppression curves, the curve with the best
699 correlation coefficient was then confirmed through a permutation test with a Bonferroni-corrected (n
700 = 6-8) significance cut-off of $p < 0.05$. ROIs that passed that permutation test were considered truly
701 suppressed (Supplementary Fig. 2).

702

703 **Statistics**

704 Graphical presentation and statistical analysis was done in Matlab. For retinal electrophysiology
705 recordings, all recorded RGCs were considered in group data. For *In-vivo* calcium imaging, only truly
706 suppressed ROIs (as described above) were considered for group data. Group data were tested for
707 normality using a Lilliefors test. Since almost all data did not pass this test we chose non-parametric
708 tests for further statistical analysis. Wilcoxon signed-rank tests were used for paired observations;
709 Wilcoxon rank-sum tests were used for independent sample testing. For regression-based analysis and
710 to identify truly suppressed ROIs in *in-vivo* calcium recordings, Pearson linear correlation was used.
711 For correlation between saccade size and normalized flash response (Fig. 5g), Spearman rank
712 correlation was used. A χ^2-test for proportions was used to compare proportions of suppressed ROIs
713 across experiments (Fig. 7b). For all tests p-value cutoffs were Bonferroni-corrected for multiple testing,
714 when necessary and $p < 0.05$ was considered as significance cut-off.

715

Data Availability

The data that support the findings of this study are available from the corresponding author upon request.

References

1. Zuber, B. L. & Stark, L. Saccadic suppression: Elevation of visual threshold associated with saccadic eye movements. *Exp Neurol* **16**, 65–79 (1966).

2. Beeler, G. W. Visual threshold changes resulting from spontaneous saccadic eye movements. *Vision Res* **7**, 769–775 (1967).

3. Burr, D. C., Morrone, M. C. & Ross, J. Selective suppression of the magnocellular visual pathway during saccadic eye movements. *Nature 1994 371:6497* **371**, 511–513 (1994).

4. Bremmer, F., Kubischik, M., Hoffmann, K. P. & Krekelberg, B. Neural dynamics of saccadic suppression. *Journal of Neuroscience* **29**, 12374–12383 (2009).

5. Hafed, Z. M. & Krauzlis, R. J. Microsaccadic suppression of visual bursts in the primate superior colliculus. *Journal of Neuroscience* **30**, 9542–9547 (2010).

6. Idrees, S., Baumann, M. P., Franke, F., Münch, T. A. & Hafed, Z. M. Perceptual saccadic suppression starts in the retina. *Nat Commun* **11**, 1–19 (2020).

7. Easter, S. S. & Gregory Nicola, J. N. The Development of Eye Movements in the Zebrafish (Danio rerio). *Dev Psychobiol* **31**, 267–276 (1997).

8. Schoonheim, P. J., Arrenberg, A. B., Del Bene, F. & Baier, H. Optogenetic localization and genetic perturbation of saccade-generating neurons in Zebrafish. *Journal of Neuroscience* **30**, 7111–7120 (2010).

9. Bollmann, J. H. The Zebrafish Visual System: From Circuits to Behavior. *https://doi.org/10.1146/annurev-vision-091718-014723* **5**, 269–293 (2019).

10. Baumann, M. P., Idrees, S., Münch, T. & Hafed, Z. Selective peri-saccadic suppression of low spatial frequencies is a visual phenomenon. *J Vis* **19**, 253–253 (2019).

11. Ridder, W. H. & Tomlinson, A. A comparison of saccadic and blink suppression in normal observers. *Vision Res* **37**, 3171–3179 (1997).

12. Chen, C. Y. & Hafed, Z. M. A neural locus for spatial-frequency specific saccadic suppression in visual-motor neurons of the primate superior colliculus. *J Neurophysiol* **117**, 1657–1673 (2017).

13. Michels, L. & Lappe, M. Contrast dependency of saccadic compression and suppression. *Vision Res* **44**, 2327–2336 (2004).

14. Knöll, J., Binda, P., Concetta Morrone, M. & Bremmer, F. Spatiotemporal profile of peri-saccadic contrast sensitivity. *J Vis* **11**, 15–15 (2011).

15. Bianco, I. H., Kampff, A. R. & Engert, F. Prey capture behavior evoked by simple visual stimuli in larval zebrafish. *Front Syst Neurosci* **5**, 18496 (2011).

16. Sperling, G. Temporal and Spatial Visual Masking. I. Masking by Impulse Flashes. *JOSA, Vol. 55, Issue 5, pp. 541-559* **55**, 541–559 (1965).

17. Matin, E., Clymer, A. B. & Matin, L. Metacontrast and Saccadic Suppression. *Science (1979)* **178**, 179–182 (1972).

18. Campbell, F. W. & Wurtz, R. H. Saccadic omission: Why we do not see a grey-out during a saccadic eye movement. *Vision Res* **18**, 1297–1303 (1978).

19. Idrees, S. *et al.* Suppression without inhibition: how retinal computation contributes to saccadic suppression. *Communications Biology 2022 5:1* **5**, 1–23 (2022).

20. Diamond, M. R., Ross, J. & Morrone, M. C. Extraretinal control of saccadic suppression. *J Neurosci* **20**, 3449–55 (2000).

21. Ali, M. A., Lischka, K., Preuss, S. J., Trivedi, C. A. & Bollmann, J. H. A synaptic corollary discharge signal suppresses midbrain visual processing during saccade-like locomotion. *Nature Communications 2023 14:1* **14**, 1–18 (2023).

22. Kennard, D. W., Hartmann, R. W., Kraft, D. P. & Boshes, B. Perceptual suppression of afterimages. *Vision Res* **10**, 575–585 (1970).

23. Volkmann, F. C. Human visual suppression. *Vision Res* **26**, 1401–1416 (1986).

24. Kayama, Y., Riso, R. R., Bartlett, J. R. & Doty, R. W. Luxotonic responses of units in macaque striate cortex. *https://doi.org/10.1152/jn.1979.42.6.1495* **42**, 1495–1517 (1979).

25. Ibbotson, M. R., Price, N. S. C., Crowder, N. A., Ono, S. & Mustari, M. J. Enhanced Motion Sensitivity Follows Saccadic Suppression in the Superior Temporal Sulcus of the Macaque Cortex. *Cerebral Cortex* **17**, 1129–1138 (2007).

26. Easter, S. S. & Nicola, G. N. The development of vision in the zebrafish (Danio rerio). *Dev Biol* **180**, 646–663 (1996).

27. Dehmelt, F. A. *et al.* Spherical arena reveals optokinetic response tuning to stimulus location, size, and frequency across entire visual field of larval zebrafish. *Elife* **10**, (2021).

28. Dowell, C. K., Lau, J. Y. N. & Bianco, I. H. The saccadic repertoire of larval zebrafish reveals kinematically distinct saccades that are used in specific behavioural contexts. *bioRxiv* 2023.11.07.565345 (2023) doi:10.1101/2023.11.07.565345.

29. Wang, K., Hinz, J., Zhang, Y., Thiele, T. R. & Arrenberg, A. B. Parallel Channels for Motion Feature Extraction in the Pretectum and Tectum of Larval Zebrafish. *Cell Rep* **30**, 442-453.e6 (2020).

30. Crapse, T. B. & Sommer, M. A. Corollary discharge across the animal kingdom. *Nat Rev Neurosci* **9**, 587 (2008).

31. Fukutomi, M. & Carlson, B. A. A History of Corollary Discharge: Contributions of Mormyrid Weakly Electric Fish. *Front Integr Neurosci* **14**, 561912 (2020).

32. Cavanaugh, J., Berman, R. A., Joiner, W. M. & Wurtz, R. H. Saccadic Corollary Discharge Underlies Stable Visual Perception. *Journal of Neuroscience* **36**, 31–42 (2016).

33. Idrees, S., Baumann, M. P., Franke, F., Münch, T. A. & Hafed, Z. M. Perceptual saccadic suppression starts in the retina. *Nat Commun* **11**, 1–19 (2020).

34. Rajkai, C. *et al.* Transient Cortical Excitation at the Onset of Visual Fixation. *Cerebral Cortex* **18**, 200–209 (2008).

35. Ibbotson, M. R., Crowder, N. A., Cloherty, S. L., Price, N. S. C. & Mustari, M. J. Saccadic Modulation of Neural Responses: Possible Roles in Saccadic Suppression, Enhancement, and Time Compression. *The Journal of Neuroscience* **28**, 10952 (2008).

36. Cloherty, S. L., Mustari, M. J., Rosa, M. G. P. & Ibbotson, M. R. Effects of saccades on visual processing in primate MSTd. *Vision Res* **50**, 2683–2691 (2010).

37. Hamker, F. H., Zirnsak, M., Calow, D. & Lappe, M. The Peri-Saccadic Perception of Objects and Space. doi:10.1371/journal.pcbi.0040031.

38. Volotsky, S., Vinepinsky, E., Donchin, O. & Segev, R. Long-range neural inhibition and stimulus competition in the archerfish optic tectum. *J Comp Physiol A Neuroethol Sens Neural Behav Physiol* **205**, 537–552 (2019).

39. Segev, R., Schneidman, E., Goodhouse, J. & Ii, M. J. B. Role of Eye Movements in the Retinal Code for a Size Discrimination Task. *J Neurophysiol* **98**, 1380–1391 (2007).

40. Malevich, T., Zhang, T., Baumann, M. P., Bogadhi, A. R. & Hafed, Z. M. Faster Detection of "Darks" than "Brights" by Monkey Superior Colliculus Neurons. *Journal of Neuroscience* **42**, 9356–9371 (2022).

41. Wu, W. & Hafed, Z. M. Stronger premicrosaccadic sensitivity enhancement for dark contrasts in the primate superior colliculus. *Scientific Reports 2025 15:1* **15**, 1–17 (2025).

42. Dunn, T. W. *et al.* Brain-wide mapping of neural activity controlling zebrafish exploratory locomotion. *Elife* **5**, (2016).

43. Tikidji-Hamburyan, A. *et al.* Retinal output changes qualitatively with every change in ambient illuminance. **6**, (2014).

44. Cameron, D. A. Mapping absorbance spectra, cone fractions, and neuronal mechanisms to photopic spectral sensitivity in the zebrafish. *Vis Neurosci* **19**, 365–372 (2002).

45. Vogalis, F. *et al.* Ectopic expression of cone-specific G-protein-coupled receptor kinase GRK7 in zebrafish rods leads to lower photosensitivity and altered responses. *Journal of Physiology* **589**, 2321–2348 (2011).

46. Collery, R. F., Veth, K. N., Dubis, A. M., Carroll, J. & Link, B. A. Rapid, Accurate, and Non-Invasive Measurement of Zebrafish Axial Length and Other Eye Dimensions Using SD-OCT Allows Longitudinal Analysis of Myopia and Emmetropization. *PLoS One* **9**, 110699 (2014).

822 47. Zhang, Y., Huang, R., Nörenberg, W. & Arrenberg, A. B. A robust receptive field code for optic
823 flow detection and decomposition during self-motion. *Current Biology* **32**, 2505-2516.e8
824 (2022).

825 48. Pachitariu, M. *et al.* Suite2p: beyond 10,000 neurons with standard two-photon microscopy.
826 *bioRxiv* 061507 (2017) doi:10.1101/061507.

827 49. Shainer, I. *et al.* A single-cell resolution gene expression atlas of the larval zebrafish brain.
828 (2023).

829 50. Avants, B. B. *et al.* A reproducible evaluation of ANTs similarity metric performance in brain
830 image registration. *Neuroimage* **54**, 2033–2044 (2011).

831

832

Acknowledgements

This work was funded by the Deutsche Forschungsgemeinschaft (DFG; German Research Foundation) through the Special Priority Programme: "SPP 2205 Evolutionary optimization of neural processing" (430158665; AR 1076/1-2, HA 6749/3-2, AR 1076/1-1), by the Major Research Instrumentation programme of the DFG (INST 37/1254-1 FUGG), and by the Human Frontier Science Program (HFSP) Young Investigator grant RGY0079. We want to thank all members of the Arrenberg group for fruitful discussions regarding this work, Saad Idrees for his incredible support and expertise regarding retinal electrophysiology and we want to thank Lidia García-Pradas for her excellent fish care.

Author Contributions

G.S. performed experiments in the retina and optic tectum, C.T. performed experiments in the optic tectum. G.S. and C.T. analyzed data and generated figures. T.C.H. developed the visual stimulation hardware and software. F.A.D. helped design visual stimuli and generated supplementary materials. G.S., Z.M.H. and A.B.A. designed the overall study. G.S. and A.B.A. conceived the experiments and associated analyses and wrote the manuscript. Z.M.H and A.B.A acquired funding for the project.

Competing Interests

The authors declare no competing interest.